International Journal of Nanomedicine

Dovepress
open access to scientific and medical research

Open Access Full Text Article

ORIGINAL RESEARCH

Multifunction hexagonal liquid-crystal containing modified surface TiO_2 nanoparticles and terpinen-4-ol for controlled release

This article was published in the following Dove Press journal:
International Journal of Nanomedicine
22 January 2015
Number of times this article has been viewed

Eloísa Berbel Manaia[1]
Renata Cristina Kiatkoski Kaminski[2]
Anselmo Gomes de Oliveira[1]
Marcos Antonio Corrêa[1]
Leila Aparecida Chiavacci[1]

[1]Drugs and Medicines Department, Faculty of Pharmaceutical Sciences, [2]Physical-Chemistry Department, Chemistry Institute, São Paulo State University – UNESP, Araraquara, Brazil

Abstract: Multifunctional products have been developed to combine the benefits of functional components and terpinen-4-ol (TP) delivery systems. In this way, p-toluene sulfonic acid modified titanium dioxide (TiO_2) nanoparticles and TP, an antioxidant, have been incorporated in liquid-crystalline formulations for photoprotection and controlled release of the TP, respectively. By X-ray powder diffraction and diffuse reflectance spectroscopy, we noted that using p-toluene sulfonic acid as a surface modifier made it possible to obtain smaller and more transparent TiO_2 nanoparticles than those commercially available. The liquid-crystalline formulation containing the inorganic ultraviolet filter was classified as broad-spectrum performance by the absorbance spectroscopy measurements. The formulations containing modified TiO_2 nanoparticles and TP were determined to be in the hexagonal phase by polarized light microscopy and small-angle X-ray scattering, which makes possible the controlled released of TP following zero-order kinetics. The developed formulations can control the release of TP. Constant concentrations of the substance have been released per time unit, and the modified TiO_2 nanoparticles can act as a transparent inorganic sunscreen.

Keywords: titanium dioxide, sol-gel, drug delivery, sunscreen

Introduction

Cosmetic products have been developed aiming to combine the benefits of functional ingredients with the latest technology in delivery systems.[1] Sunscreen is a class of products with many innovative formulations because consumers are looking for protection from skin cancer and other damage caused by ultraviolet A (UVA) and ultraviolet B (UVB) radiations, such as photoaging, pigmentation, wrinkling, and dryness.[2] Accordingly, formulations are developed with UVA and UVB blockers along with complementary active compounds incorporated in delivery systems to obtain differentiated multifunctional products. In this way, García-González et al used solid lipid nanoparticles containing titanium dioxide (TiO_2) and caffeine to make sunscreens free of organic absorbers. To treat skin diseases or to prevent skin cancer, solid lipid particles have been used as a vehicle for the topical administration and controlled release of caffeine for anticellulite activity and photoaging prevention.[3] Dai et al combined a photosensitive azobenzene compound with liposome encapsulated ascorbic acid (vitamin C) to promote collagen biosynthesis and prevent free radical formation. The photoisomerization of the azobenzene compound controls the release of the ascorbic acid under ultraviolet (UV) radiation and at the same time protects the skin from UV radiation.[4] Commonly, sunscreens have vitamins C and E as ingredients because they have been shown to maximize the UV protection of the skin and reverse changes induced by both chronologic and photoaging.[5]

Correspondence: Leila Aparecida Chiavacci
Drugs and Medicines Department, Faculty of Pharmaceutical Sciences of São Paulo State University – UNESP, Araraquara-Jaú Interstate Highway, Km 1, Araraquara, Brazil
Tel +55 16 3301 6966
Fax +55 16 3301 6900
Email leila@fcfar.unesp.br

Organic UV absorbers are generally photo unstable, and the preference to improve the sun protection factor and the photostability of these molecules is the use of controlled release systems, as employed with benzophenone-3,[6] oxybenzone,[7] phenylbenzimidazole sulfonic acid,[8] 2-ethylhexyl-2-cyano-3,3-diphenylacrylate, 2-ethylhexyl trans-4-methoxycinnamate, and Bis-ethylhexyloxyphenol methoxyphenyl triazine.[9] In the end of 1980s, the use of inorganic particles became popular, being presented with various types of treatment surface, as dispersions, and as micronized particles in order to enhance the photoprotection against UVA radiation and to minimize photoreactivity displayed by the organic UV filters traditionally used.[10] Inorganic UV blockers (ie, oxides) protect the skin by reflecting, scattering, or absorbing UV radiation and are photostable, nonallergenic,[11,12] and provide a large UV-spectrum coverage.[12] However, they tend to be opaque and white when applied on the skin and consequently are unacceptable for cosmetic use. Therefore, to be used in sunscreens, inorganic compounds such as titanium dioxide and zinc oxide must be present at a controlled size,[13] to promote more efficient uniform protection against UV radiation, to prevent visible light scattering[14] and hence many of them have surface modifiers[15,16] to impede aggregation[11] of the particles caused by electrostatic effects. Examples of surface modifiers are dimethicone, silica,[12] alumina, aluminum stearate,[11] aluminum oxide, simethicone, stearic acid,[15] solid lipid microparticles,[3] and polyaspartic acid.[16] Recently, we demonstrated the efficiency of p-toluene sulfonic acid (PTSH) to control the size, shape, and aggregation of TiO_2 nanoparticles obtained by the sol-gel process.[17,18]

Besides sunscreen application, TiO_2 have also been used in different devices for gene or drug delivery, as well as other inorganic nanoparticles. Song et al have demonstrated the use of TiO_2 nanotubular structure with a hydrophobic cap which prevents uncontrolled leaching of the hydrophilic drug into an aqueous environment.[19] Ghedini et al have shown the feasibility of TiO_2-based matrices with high surface area and well-defined mesoporous textures for the sustained release of ibuprofen.[20] In the literature, it was reported that a nontoxic TiO_2 nanoparticle-based system conjugated with a monoclonal antibody could be applied for therapeutic purposes in pancreatic cancer.[21] Recently, the first report on the production of bifunctional three-phase metal oxide–Ag_3PO_4–graphene composite materials with improved photocatalytic and antibacterial properties was reported.[22] TiO_2 as well as Fe_2O_3, SiO_2, Co, and Au have also been associated in a new class of materials with a distinctive core–void–shell configuration called yolk/shell nanoparticles (YSNs). For example, Fe_3O_4–SiO_2 YSNs show both high drug loading capacity and magnetization strength; Co–Au YSNs have been employed as biocompatible nonviral gene transport vehicles; and titania-based yolk/shell microspheres are verified by cell-viability assays to be noncytotoxic.[23] Despite the possibility of using TiO_2 as a drug carrier, for topical application it is better to use in skin formulations with optimal sensorial aspects. In this work, we used TiO_2 nanoparticles as a UV blocker and chose another system for drug delivery control aiming to optimize sensorial aspects.

There are many systems used as delivery vehicles, including liquid-crystalline formulations in lamellar, hexagonal, and cubic phases (according to the arrangement of the surfactant molecules). These nanostructured systems present advantages such as low cost, simple preparation, and hydrophilic/hydrophobic component incorporation capacity due to the amphiphilic character of the surfactant molecules.[24] Among these liquid-crystalline phases, the hexagonal mesophases are regarded as promising terpinen-4-ol (TP) delivery vehicles.[25–27] The hexagonal phase can be denoted as long cylinders: each one consists of rod-shaped micelles surrounded by a continuous water region. In this way, hydrophilic molecules can be embedded within the aqueous domains, and hydrophobic molecules can be embedded by direct interaction within their hydrophobic compartments.[25]

Currently, natural antioxidants are demanded in topical applications. The essential oil derived from *Melaleuca alternifolia*, or tea tree oil (TTO), presents a mixture of compounds, mainly monoterpenes and their corresponding alcohols. The active component TP, which exhibits the highest concentration in TTO,[28] has gained attention because of its antibacterial,[29] antifungal,[30] antiviral, anti-inflammatory,[31,32] antioxidant,[33] and antitumoral (melanoma)[34] properties.

The aim of the present work is to develop liquid-crystalline formulations containing (i) surface-modified transparent TiO_2 nanoparticles obtained from a sol-gel process to protect the skin against UVA and UVB radiation and (ii) TP as an antioxidant to be released via controlled delivery.

Materials and methods

TiO_2 nanoparticle synthesis

To obtain surface-modified TiO_2 nanoparticles, we used a recently developed thermoreversible sol-gel transition described elsewhere.[17,18] Briefly, TiO_2 nanoparticles were prepared by drop by drop addition of a PTSH aqueous solution to a solution of titanium tetraisopropoxide in isopropanol under continuous magnetic stirring at room temperature. The clear suspension was placed in a closed glass in the oven

at 60°C for 18 hours. We have used the nominal hydrolysis ratio (H=[H_2O]/[Ti]) of 2.3 and the nominal acidity ratio (P=[PTSH]/[Ti]) of 0.2. The xerogel was formed after solvent evaporation at 60°C.

Preparation of the liquid-crystalline formulations

Liquid-crystalline formulations were prepared with PPG-5 Ceteth 20 (Procetyl AWS; Croda, Campinas, Brazil) as the surfactant, isopropyl palmitate as the oil phase, and ultrapure water (H_2O) at a ratio of 48:30:22 (w:w:w). We added 30% (considering the weight) of modified TiO_2 nanoparticles to the formulations, and in the oil phase, 1% (F1) and 5% (F5) of TP were used (Sigma-Aldrich Co., St Louis, MO, USA). Due to the hydrophobic nature of TP, its percentage was subtracted during the oil phase. Table 1 displays the formulation composition as well as their sample notation. All the components were mixed using mechanical stirring at 7,000 rpm at 25°C, and the pH levels of the formulations were adjusted to between 5 and 7.

Physical-chemistry characterization

X-ray diffraction

The average size of TiO_2 xerogel and commercial TiO_2 (Sachtleben, Krefeld, Germany) crystallite were determined by X-ray diffraction (XRD) with a Siemens D5000 diffractometer, using the Cu Kα radiation, λ=1.5418 Å. This radiation level was selected by a using graphite monochromator and a fixed divergence slit of 1/8° in a Bragg–Brentano configuration. The diffraction intensity data were measured in the range of 2θ between 10° and 80° by the step counting method (step 0.02° and time 3 seconds).

Transmission electron microscopy

The transmission electron micrographs were recorded at the Brazilian Nanotechnology National Laboratory – CNPEM/ABTLuS (LNNano), using a JEOL3010 HRTEM (high-resolution transmission electron microscope). Samples were prepared by placing a drop of TiO_2 xerogel suspension on a perforated carbon-coated copper grid.

Table 1 Composition of the liquid-crystalline formulations and release constants (K_0p and K_0q) for formulations F1 and F5 (data are mean ± SEM, n=6)

Sample notation	F1	F5
PC (% w/w)	48	48
IP (% w/w)	29	25
H_2O (% w/w)	22	22
TiO_2 added to the formulations (% w/w)	30	30
TP (% w/w)	1	5
Release constant K_0p [% (μg) h^{-1}]	1.12±0.07	1.0±0.10
Release constant K_0q (μg cm^{-2} h^{-1})	20.8±0.71	97.3±1.59

Abbreviations: h, hours; IP, isopropyl palmitate; PC, PPG-5 Ceteth 20; SEM, standard error of the mean; TP, terpinen-4-ol; w, weight.

Diffuse reflectance spectroscopy

First, we prepared a liquid-crystalline formulation with the same composition and parameters of the other ones containing 15% commercial TiO_2 (Sachtleben) as a comparison formulation. The diffuse reflectance spectra of the formulations were obtained with a Cary spectrophotometer equipped with a HARRICK attachment. The reflectance measurements of the formulations containing 15% commercial TiO_2 and 30% xerogel TiO_2 were referenced to the MgO optical standard in the visible spectrum (400–700 nm).

UV absorption spectroscopy

The measurement of the spectral absorption of UV radiation (290–400 nm) through a substrate before and after application of the sunscreen preparation was performed with the liquid-crystalline formulation with (30%) and without modified TiO_2 nanoparticles. The substrate used was 3M Transpore taped in a single layer on clean 2 mm thick quartz slides. Approximately 2 mg/cm^2 of the formulation was uniformly spread using a finger glove. The samples were allowed to air dry for 20 minutes as performed in the literature,[35,36] to let the formulation break and prevent an inaccurate measurement, and the plates were placed inside the UV-2000S Ultraviolet Transmittance Analyzer. Before running the sample, the blank slide was loaded into the sample holder for the blank scan. Irradiation took place at nine different areas of the substrate. The experiment was performed in triplicate. The spectral data were processed by the Labsphere software and the critical wavelength was calculated.

Polarized light microscopy

Microscopic analyses were carried out at 23°C using a polarizing light microscope (Carl Zeiss Jenamed 2) equipped with a digital camera to determine the liquid-crystalline arrangement. The samples (F1 and F5) were placed on a glass slide and covered with a cover slip.

Small-angle X-ray scattering

Scatterings measurements of the formulations F1 and F5 were performed at the SAXS1 beamline of the National Laboratory of Synchrotron Light (LNLS, Campinas, Brazil). The LNLS beamline is equipped with a monochromator (λ=1.549 Å), a vertical detector localized 579.395 mm from the sample, and a multichannel analyzer to register the scattering intensity $I(q)$ as

a function of the scattering vector, q. Data were normalized to accommodate the beam decay, detector sensitivity, and sample transmission. The parasitic scattering intensity (cell windows and air) was subtracted from the total scattering intensity.

In vitro release studies

The in vitro TP release was evaluated using Franz diffusion cells where a 0.45 mm (pore size) cellulose acetate membrane was positioned between the donor compartment (area exposed to donor compartment 1.77 cm^2) containing the TP formulations and the acceptor compartment (7 mL acceptor phase: aqueous solution of NaCl 0.9% with 1% of Tween 80 to ensure sink conditions). The experiment was carried out using six diffusion cells (n=6) under constant stirring (300 rpm) by a magnetic bar at 32.5°C±0.5°C (maintained by a surrounding water jacket) over 12 hours. The time intervals for sample collection were: 0.5, 1.0, 2.0, 4.0, 6.0, 8.0, 10.0, and 12 hours. To eliminate the false volume of the equipment, we discarded the initial 0.8 mL followed by collection of 2.0 mL during the receptor phase to quantify the TP. These volumes (2.8 mL) of the acceptor phase were immediately replaced with fresh solution. The samples used were formulations F1 and F5 as well as TP incorporated in propylene glycol (PG) at concentrations of 1% and 5% to evaluate differences of the TP released from the designed formulations and from solvent (PG). TP PG solutions were prepared simply by mixing TP with the solvent.

Analytical method

TP released in the acceptor phase was quantified by high-performance liquid chromatography. The column XDB C18, 5 mm, 250×4.6 mm (Agilent Zorbax Eclipse) was employed at 25°C. The mobile phase used was acetonitrile:water 55:45 (v/v) with a flow rate of 2.00 mL/min. An aliquot of 30 µL was injected to the column, and the UV-absorbance at 200 nm was measured as used in similar study.[37]

Data analysis

In the TP release experiments described, the acceptor phase was routinely diluted due to sample removal and replacement with equal volumes of fresh solution. Thus, the cumulative TP released (Q_t) was calculated by equation 1:[38]

$$Q_t = V_a \cdot C_t + \sum_{i=0}^{t-1} V_s \cdot C_i \quad (1)$$

where C_t is the substance TP concentration in the acceptor phase at each sampling time, C_i is the substance TP concentration of the ith sample, and V_a and V_s are the relative volumes of the acceptor phase and the sample, respectively. The data were expressed as the cumulative substance TP released per unit of membrane surface area, Qt/S (S=1.77 cm^2) and the percentage released was calculated.

Results

Characterization of TiO_2 nanoparticles and their incorporation in liquid-crystalline systems

First, we compared the average nanocrystallite size of the xerogel obtained by the sol-gel process with the commercial TiO_2 estimated from the [1 0 1] Bragg peak of XRD traces using Scherrer equation 2:[39–41]

$$D = \frac{\kappa\lambda}{\beta\cos\theta} \quad (2)$$

where D is the crystallite size; κ is a constant (shape factor), λ is the X-ray wavelength, β is the full-width-at-half-maximum of a characteristic diffraction peak, and θ is the diffraction angle. It was assumed that peak broadening is essentially due to size effects. The calculated XRD crystallite size of the surface modified TiO_2 with PTSH and the commercial TiO_2 was 0.7 nm and 56.9 nm, respectively.

The transmission electron microscopy (TEM) image was recorded to determine the size of TiO_2 nanoparticles. Figure 1 shows the TEM image of the TiO_2 xerogel. The average nanoparticle size was about 16 nm.

Diffuse reflectance spectroscopy has been used to analyze the transparency of diverse materials in the visible spectrum.[42] Figure 2 presents the visible diffuse reflectance spectra of liquid-crystalline formulations containing 15% commercial TiO_2 and 30% xerogel obtained by the sol-gel

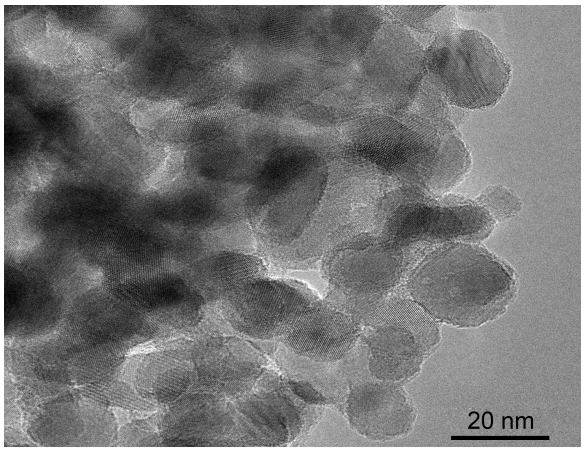

Figure 1 TEM image of TiO_2 nanoparticles obtained by sol-gel process.
Abbreviations: TEM, transmission electron microscopy; TiO_2, titanium dioxide.

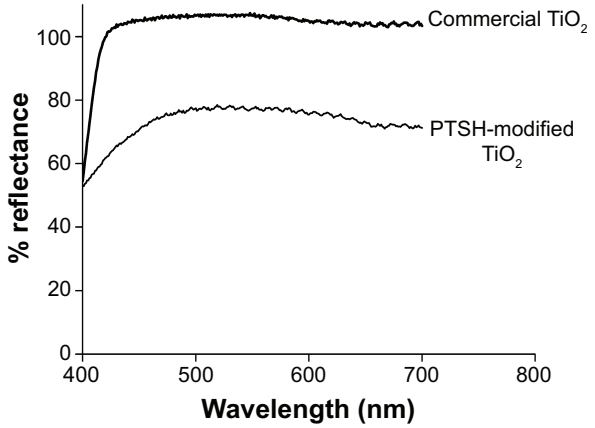

Figure 2 Visible diffuse reflectance spectra of liquid-crystalline formulations containing 15% commercial TiO_2 and 30% PTSH-modified TiO_2 nanoparticles.
Abbreviations: PTSH, p-toluene sulfonic acid; TiO_2, titanium dioxide.

process. Xerogel nanoparticle formulations displayed lower reflectance (about 70%) in the visible region compared with commercial TiO_2 formulations (about 100%).

Figure 3 shows the absorbance spectra of liquid-crystalline formulations with and without modified TiO_2 nanoparticles. It is important to note that the modified TiO_2 nanoparticles are solely responsible for the UV protection in the formulations analyzed in this work. The liquid-crystalline system without TiO_2 does not affect the absorption in the range of UVB and UVA of TiO_2, presenting absorbance about 0 in the UVA and UVB regions. Figure 3 also appoints the critical wavelength (λ_c) of the liquid-crystalline formulation with modified TiO_2 nanoparticles, 377.11 nm being the wavelength which comprises 90% of the area under the spectrum from 290 nm to 400 nm.

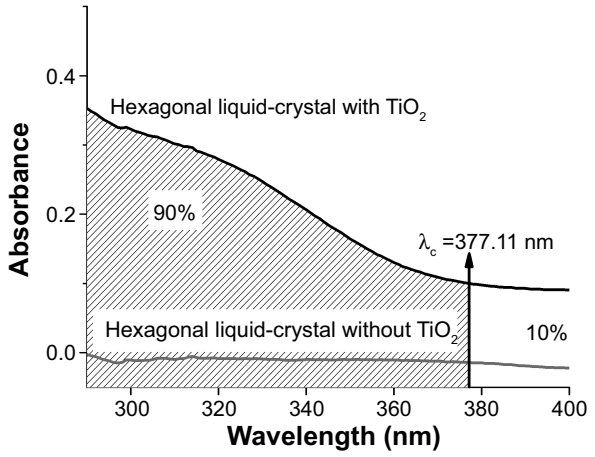

Figure 3 Absorbance spectra of liquid-crystalline formulations with and without TiO_2 nanoparticles.
Notes: λ_c of the formulation containing TiO_2 is appointed over the arrow which traces 90% of the area under the spectrum from 290 to 400 nm.
Abbreviations: λ_c, critical wavelength; TiO_2, titanium dioxide.

To characterize the liquid-crystalline structures of the formulations, we used polarized light microscopy for preliminary identification[43] and small-angle X-ray scattering (SAXS) measurements to confirm the liquid-crystalline phase. Figure 4 shows the photomicroscopic images of the formulation F1 containing TP and the SAXS curves of the F1 and F5 formulations. We can identify from the photomicrography the hexagonal liquid-crystalline structure indicated by the fanlike texture observed in Figure 4B.[25,44] To confirm the hexagonal phase in the formulations, SAXS curves were performed.[45] It is possible to calculate structural parameters and to determine the liquid-crystalline phase according to the relationship between the distances of the Bragg peaks on the scattering vector (q).[46] The equation $d=2\pi/q_{max}$, where q_{max} is the q value at the peak intensity $I(q)$, was used to calculate the correlation distance between the scattering objects.[44] The relation between the distance d calculated for each peak must conform to the relation $\sqrt{1}:\sqrt{3}:\sqrt{4}$ for the hexagonal phase.[47,48] Figure 4A shows the SAXS profile: peaks identified with pointers indicate the presence of hexagonal structure in the F1 and F5 formulations, confirming the microscopy results.

Drug release profile of TP in liquid-crystalline formulation

The in vitro TP release experiments were performed with the formulations F1 and F5 and also with the TP dissolved in PG at concentrations of 1% and 5% to evaluate the differences in the percentage released from the structured formulations and from the solvent. Figure 5A presents the percentage of TP released over time. The percent of the released TP up to the full 12 hours of the in vitro test was approximately 13% for F1 and F5 formulations from the liquid-crystalline phase. However, the PG samples released approximately 30% and 40% with 1% and 5% TP, respectively. Figure 5B shows the cumulative TP released per membrane unit area over time of the F1 and F5 formulations. We can observe a linear behavior for both formulations, and the formulation with higher concentration of TP (F5) presented a higher rate of TP release from the formulation per unit time.

Discussion

The size of the TiO_2 particles is crucial in sunscreen products because this parameter affects both the range of UV protection and the intensity of visible light reflection by the particles on the skin. The crystallite size of the xerogel calculated by the Scherrer equation is almost 100 times smaller than those commercially available, and this characteristic is

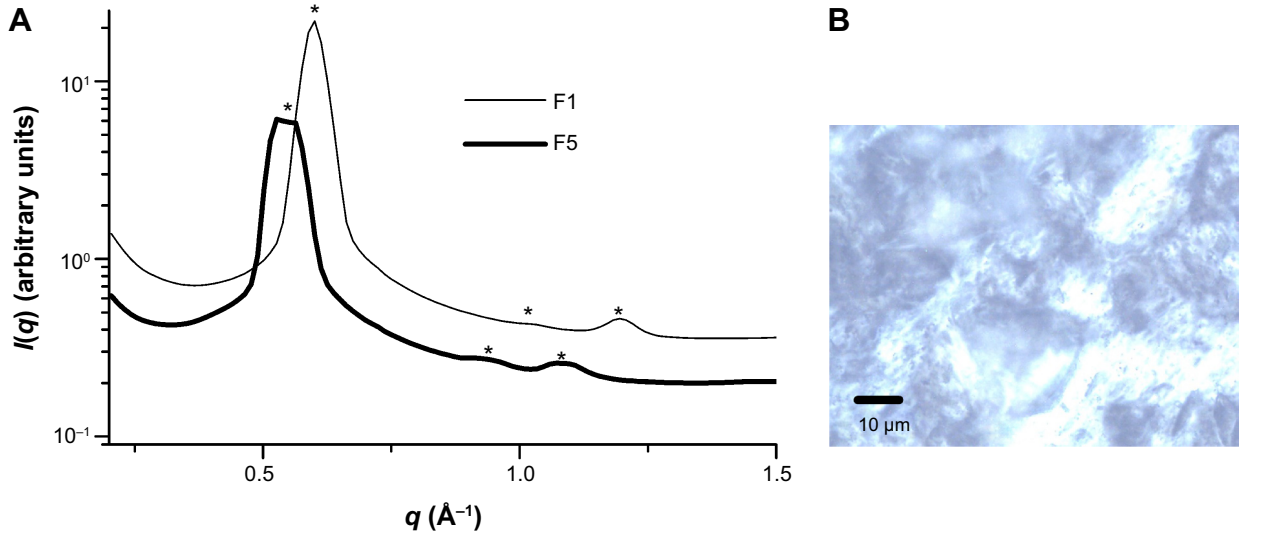

Figure 4 SAXS curves and polarized light micrographs of liquid-crystalline formulations (**A**) F1 and F5 and (**B**) F1.
Note: *Appoints the peaks related to the hexagonal phase.
Abbreviations: *I*(*q*), scattering intensity; SAXS, small-angle X-ray scattering.

beneficial for the incorporation of the xerogel in cosmetic formulations, improving transparency and smoothness. By TEM it was possible to visualize the real size of the TiO_2 nanoparticles obtained by the sol-gel process, which presented an average size about 16 nm, which is significantly smaller than that used previously in commercial sunscreen products without nanomaterials (size > 100 nm).[49] It is important to clarify that the size shown by TEM (average size, about 16 nm) takes into account the aggregation of the TiO_2 nanocrystallites and the size obtained by XRD (about 0.7 nm), is related to the crystallite size; thus in this case, they can not be compared. The diffuse reflectance spectroscopy showed that the xerogel nanoparticles formulations presented higher transparency than those commercially available. This is due to the size difference between the xerogel nanoparticles and the commercial TiO_2 particles, as determined by the XRD data and TEM. Therefore, TiO_2 xerogel nanoparticles are promising materials for sunscreen products.

An essential requirement for the development of effective sunscreen products is protection throughout the whole UV range (290–400 nm) of sunlight.[50] There are numerous testing methods in vivo and in vitro to define their UV protection efficacy. The sunscreen in vitro tests are based on absorbance (calculated from transmittance) or reflectance measurements. The curves obtained can show two important attributes: the amplitude of the absorbance curves, which

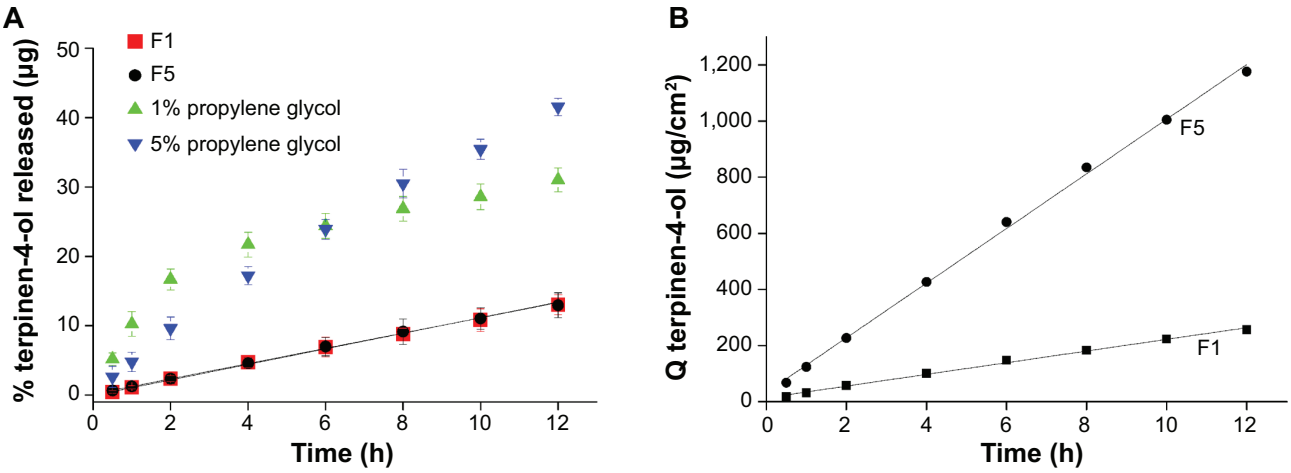

Figure 5 Terpinen-4-ol release profiles of F1 and F5 formulations.
Notes: (**A**) % (µg) plotted versus time comparing TP (1% and 5%) incorporated in propylene glycol and (**B**) Q terpinen-4-ol (µg/cm²) plotted versus time (data are mean ± SD, n=6). The lines on both graphs represent the zero-order regression line.
Abbreviations: h, hours; SD, standard deviation; TP, terpinen-4-ol.

indicates the protection degree, and the shape of the curves, which underlines the protection capability in different spectral regions.[51] Among the in vitro methodologies, the critical wavelength method proposed by Diffey is based on the absorbance spectrum reduced to a single index by means of UV substrate spectrophotometry. This method, unlike the in vivo ones, does not provide UVA-induced acute or chronic skin damage to determine the protection spectra of the sunscreen against sunlight.[52] The λ_c is determined when the area under the spectrum from 290 nm (the approximate lower wavelength limit of terrestrial sunlight) to λ_c is 90% of the integral of the absorbance spectrum from 290 to 400 nm.[53] The λ_c of the formulation was higher than 370 nm; thus, the formulation is classified as broad-spectrum protection. Importantly, the λ_c value is determined by the shape of the absorbance curve, not by its amplitude, so the application quantity and other undesired variables characteristic of the in vitro method do not affect the result. In addition, λ_c determination does not promote the erroneous notion of UVB and UVA as separate entities, but rather as part of a continuous electromagnetic spectrum.[52] It is important to remark that it is known that TiO_2 blocks UV radiation physically by scattering and reflecting the incoming radiation and chemically by absorbing it.[54] Thus, this method evaluates only the chemical activity of TiO_2.

The organized structure of the drug delivery system is extremely important to understand the release profile of the devices applied in drug-controlled release. As shown in Figure 4, the concentration of TP does not drastically affect the differences during the liquid-crystalline phase. Additionally, the SAXS curves are similar in both peak shape and broadness. Interestingly, these liquid-crystalline formulations, which contained TP and modified surface TiO_2 nanoparticles, can maintain an organized hexagonal structure, as reported previously.[55]

The data of the TP released from the solvent (PG) shown in Figure 5A can be fitted with the exponential equation $y=a(1-e^{-bx})$, initially showing an abrupt increase of the TP released, then tending toward the saturation of the acceptor phase. When TP was dissolved in PG, the release rate was only influenced by the gradient concentration of TP in the sample and the acceptor compartments of the in vitro release system. Thus, as expected, the solution with a higher TP concentration was released more quickly, whereas a lower concentration formulation released more slowly, as observed in Figure 5A. On the other hand, regardless of the TP concentration, when the organized system is present, the release rate was much lower than for TP dissolved in PG. In these cases, the TP graph obtained from the organized systems can be fitted with the linear equation $y=ax+b$, which exhibit the same amount of TP released over the time. This profile clearly shows the contribution of the structured vehicle in the controlled release of TP. We can conclude that the amount of TP transported across the membrane was limited by the vehicle in which TP was incorporated, not by the membrane itself. TP diffusion within the mesophase is related by two factors: the physical factor, which results from cylindrical obstacles formed by the arrangement of surfactant molecules, and the chemical factor, which results from the interactions with the surfactant–oil phase interface or with the oil phase itself.

Detailed analysis of the TP released shows that although the presence of the structured vehicle is the main factor controlling the entire release process, the TP concentration also has an important role in this release; making it faster with increasing TP concentration in the structured vehicle. Accordingly, the higher the TP percentage incorporated into the formulation, the higher the amount of TP released from the formulation per unit time, the higher the difference of TP gradient concentration between the donor and the acceptor compartment, and the higher the TP permeation through the membrane.

The kinetic data can be analyzed by mathematical models. The zero-order kinetic can describe the release of TP by the following equation:

$$Qt = Q_0 + K_0 t \quad (3)$$

where Qt is the amount of TP release in time t, Q_0 is the initial amount of TP in the solution, and K_0 is the zero-order release constant.[56] This configuration is ideal for achieving prolonged release of TP. In fact, the TP released from the liquid-crystalline formulations (containing TP at 1% and 5%) followed zero-order kinetics (correlation coefficient =0.9963 and 0.9984 for F1 and F5 formulations, respectively), indicating a constant TP release versus time.[57] Therefore, it was possible to calculate K_0 of F1 and F5 formulations using Equation 3. Table 1 notes that the release constants for formulations F1 and F5 are K_0p and K_0q, where p is attributed to the percentage of TP released versus time and q is attributed to the quantity of TP released per membrane unit area versus time. Looking at the K_0p values, we noted that these values are very close, showing that the structured formulations are able to control the release velocity independent of the TP quantity incorporated into the formulations. The long-time release profile of TP from the organized system was slower than the free substance permeation through the membrane in the in vitro release process. When we analyze the values

of the K_0q, it is possible to observe that the value of K_0q for the formulation containing 5% of TP is approximately five times higher than the K_0 of the formulation containing 1% of TP. These values clearly show that the higher the percentage incorporated into the system, the higher the release rate will be due to the increase of the gradient concentration in the donor compartment. Thus, it is possible to modulate the amount of TP released per membrane area unit/time, which changes the percentage of TP incorporated into the formulations.

Conclusion

The PTSH surface-modified nanoparticles obtained by the sol-gel process have a controlled size and permit the creation of cosmetic formulations that are more transparent than those commercially available. The homogeneous macroscopic aspect of the liquid-crystalline formulation composed by PPG-5 Ceteth 20, isopropyl palmitate, and ultrapure water indicates an efficient process for incorporating modified TiO_2 nanoparticles and TP. The hexagonally organized structure was maintained after adding modified TiO_2 nanoparticles and TP. In the two concentrations of the TP incorporated (1% and 5%), the formulations release the same amount of TP per unit time, controlling the release according to the zero-order kinetics model. For this reason, these systems showed that it is possible to control the amount of TP released according to the percentage of TP incorporated in the formulations. The results obtained in this work show the possibility of creating new alternatives for systems used as vehicles for photoprotection and can aggregate knowledge for future development of multifunctional systems that aim to protect the skin against harmful effects of the sun and control the delivery of biological active molecules.

Acknowledgments

The authors thank the LNLS (project number: 12462) for SAXS measurements, Marina Magnani for TEM measurements at LNNano, and FAPESP, CNPq, and PADC/FCF-UNESP for the financial support. We would also like to thank Professors André R. Baby, Celso V Santilli, and Sandra H Pulcinelli for allowing us to use their laboratory (USP/São Paulo and UNESP/Araraquara) during the UV absorption spectroscopy, diffuse reflectance spectroscopy, and polarized light microscopy measurements.

Disclosure

The authors report no conflicts of interest in this work.

References

1. Patravale VB, Mandawgade SD. Novel cosmetic delivery systems: an application update. *Int J Cosmet Sci*. 2008;30(1):19–33.
2. Wang SQ, Balagula Y, Osterwalder U. Photoprotection: a review of the current and future technologies. *Dermatol Ther*. 2010;23(1):31–47.
3. García-González CA, Sampaio da Sousa AR, Argemí A, et al. Production of hybrid lipid-based particles loaded with inorganic nanoparticles and active compounds for prolonged topical release. *Int J Pharm*. 2009; 382(1–2):296–304.
4. Dai Y-Q, Qin G, Geng S-Y, Yang B, Xu Q, Wang J-Y. Photo-responsive release of ascorbic acid and catalase in CDBA-liposome for commercial application as a sunscreen cosmetic. *RSC Advances.* 2012;2:3340–3346.
5. Gianeti MD, Gaspar LR, de Camargo FB Jr, Campos PM. Benefits of combinations of Vitamin A, C and E derivatives in the stability of cosmetic formulations. *Molecules*. 2012;17:2219–2230.
6. Daoud-Mahammed S, Agnihotri SA, Bouchemal K, Kloeters S, Couvreur P, Gref R. Efficient loading and controlled release of benzophenone-3 entrapped into self-assembling nanogels. *Curr Nanosci*. 2010;6: 654–665.
7. Sanad RA, Abdelmalak NS, Elbayoomy TS, Badawi AA. Formulation of a novel oxybenzone-loaded nanostructured lipid carriers (NLCs). *AAPS Pharm Sci Tech*. 2010;11(4):1684–1694.
8. Gomaa YA, El-Khordagui LK, Boraei NA, Darwish IA. Chitosan microparticles incorporating a hydrophilic sunscreen agent. *Carbohydr Polym.* 2010;81(2):234–242.
9. Lacatusu I, Badea N, Murariu A, Meghea A. The encapsulation effect of UV molecular absorbers into biocompatible lipid nanoparticles. *Nanoscale Res Lett*. 2011;6(1):73.
10. Shaath NA. *The Encyclopedia of Ultraviolet Filter*. 1st ed. Carol Stream: Allured Pub Corp; 2007.
11. Nasu A, Otsubo Y. Effects of polymeric dispersants on the rheology and UV-protecting properties of complex suspensions of titanium dioxides and zinc oxides. *Colloids Surf A.* 2008;326(1–2):92–97.
12. Hexsel CL, Bangert SD, Hebert AA, Lim HW. Current sunscreen issues: 2007 Food and Drug Administration sunscreen labelling recommendations and combination sunscreen/insect repellent products. *J Am Acad Dermatol*. 2008;59(2):316–323.
13. Serpone N, Dondi D, Albini A. Inorganic and organic UV filters: Their role and efficacy in sunscreens and suncare product. *Inorganica Chim Acta.* 2007;360:794–802.
14. Mitchnick MA, Fairhurst D, Pinnell SR. Microfine zinc oxide (Z-cote) as a photostable UVA/UVB sunblock agent. *J Am Acad Dermatol*. 1999; 40(1):85–90.
15. Stiller S, Gers-Barlag H, Lergenmueller M, et al. Investigation of the stability in emulsions stabilized with different surface modified titanium dioxides. *Colloids Surf A.* 2004;232(2–3):261–267.
16. Andre V, Rieger J, Debus H; inventor; Basf Ag, assignee. Surface-modified metal oxides useful in cosmetics comprise nanoparticulate aluminum, cerium, iron, titanium, zinc or zirconium oxides coated with polyaspartic acid. United States Patent US 2007218019-A1, 2007 Set 20.
17. Kaminski RCK, Pulcinelli SH, Judeinstein P, Meneau F, Briois V, Santilli CV. Thermo-reversible sol−gel transition of surface modified titanium poly oxo building blocks. *J Phys Chem C*. 2009;114(3): 1416–1423.
18. Kaminski RCK, Pulcinelli SH, Santilli CV, Meneau F, Blanchandin S, Briois V. Thermo-reversible sol–gel transition of TiO_2 nanoparticles with surface modified by p-toluene sulfonic acid. *J Eur Ceram Soc.* 2010;30(2):193–198.
19. Song YY, Schmidt-Stein F, Bauer S, Schmuki P. Amphiphilic TiO_2 nanotube arrays: an actively controllable drug delivery system. *J Am Chem Soc*. 2009;131(12):4230–4232.
20. Ghedini E, Nichele V, Signoretto M, Cerrato G. Structure-directing agents for the synthesis of TiO(2)-based drug-delivery systems. *Chemistry*. 2012;18(34):10653–10660.
21. Sette A, Spadavecchia J, Landoulsi J, et al. Development of novel anti-Kv 11.1 antibody-conjugated PEG-TiO_2 nanoparticles for targeting pancreatic ductal adenocarcinoma cells. *J Nanopart Res*. 2013;15:2111.

22. Yang X, Qin J, Jiang Y, Li R, Li Y, Tang H. Bifunctional TiO_2/Ag_3PO_4/graphene composites with superior visible light photocatalytic performance and synergistic inactivation of bacteria. *RSC Adv.* 2014;4:18627–18636.
23. Liu J, Qiao SZ, Chen JS, Lou XW, Xing X, Lu GQ. Yolk/shell nanoparticles: new platforms for nanoreactors, drug delivery and lithium-ion batteries. *Chem Commun (Camb)*. 2011;47(47):12578–12591.
24. Cohen-Avrahami M, Libster D, Aserin A, Garti N. Penetratin-induced transdermal delivery from H(II) mesophases of sodium diclofenac. *J Control Release*. 2012;159(3):419–428.
25. Garti N, Hoshen G, Aserin A. Lipolysis and structure controlled drug release from reversed hexagonal mesophase. *Colloids Surf B Biointerfaces*. 2012;94:36–43.
26. Libster D, Aserin A, Garti N. Interactions of biomacromolecules with reverse hexagonal liquid crystals: drug delivery and crystallization applications. *J Colloid Interface Sci*. 2011;356(2):375–386.
27. Cohen-Avrahami M, Aserin A, Garti N. H(II) mesophase and peptide cell-penetrating enhancers for improved transdermal delivery of sodium diclofenac. *Colloids Surf B Biointerfaces*. 2010;77(2):131–138.
28. Sun LM, Zhang CL, Li P. Characterization, antibiofilm, and mechanism of action of novel PEG-stabilized lipid nanoparticles loaded with terpinen-4-ol. *J Agric Food Chem*. 2012;60(24):6150–6156.
29. Burt S. Essential oils: their antibacterial properties and potential applications in foods – a review. *Int J Food Microbiol*. 2004;94(3):223–253.
30. Hammer KA, Carson CF, Riley TV. Antifungal effects of *Melaleuca alternifolia* (tea tree) oil and its components on Candida albicans, Candida glabrata and Saccharomyces cerevisiae. *J Antimicrob Chemother*. 2004;53(6):1081–1085.
31. Bakkali F, Averbeck S, Averbeck D, Idaomar M. Biological effects of essential oils – A review. *Food Chem Toxicol.* 2008;46(2):446–475.
32. Hammer KA, Carson CF, Riley TV, Nielsen JB. A review of the toxicity of *Melaleuca alternifolia* (tea tree) oil. *Food Chem Toxicol*. 2006;44(5):616–625.
33. Kim HJ, Chen F, Wu C, Wang X, Chung HY, Jin Z. Evaluation of antioxidant activity of Australian tea tree (*Melaleuca alternifolia*) oil and its components. *J Agric Food Chem*. 2004;52(10):2849–2854.
34. Calcabrini A, Stringaro A, Toccacieli L, et al. Terpinen-4-ol, the main component of *Melaleuca alternifolia* (tea tree) oil inhibits the in vitro growth of human melanoma cells. *J Invest Dermatol*. 2004;122(2):349–360.
35. Springsteen A, Yurek R, Frazier M, Carr KF. In vitro measurement of sun protection factor of sunscreens by diffuse transmittance. *Anal Chim Acta.* 1999;380:155–164.
36. Bleasel MD, Aldous S. In vitro evaluation of sun protection factors of sunscreen agents using a novel UV spectrophotometric technique. *Int J Cosmet Sci*. 2008;30(4):259–270.
37. Nielsen JB, Nielsen F. Topical use of tea tree oil reduces the dermal absorption of benzoic acid and methiocarb. *Arch Dermatol Res*. 2006;297(9):395–402.
38. Sintov AC, Botner S. Transdermal drug delivery using microemulsion and aqueous systems: influence of skin storage conditions on the in vitro permeability of diclofenac from aqueous vehicle systems. *Int J Pharm*. 2006;311(1–2):55–62.
39. Mandjoub N, Allen NS, Kelly P, Vishnyakov V. SEM and Raman study of thermally treated TiO_2 anatase nanopowders: Influence of calcination on photocatalytic activity. *J Photochem Photobiol A.* 2010;211(1):59–64.
40. Ali M, Basu P. Mechanochemical synthesis of nano-structured TiC from TiO_2 powders. *J Alloys Compd.* 2010;500(2):220–223.
41. Kaminski RC, Pulcinelli SH, Craievich AF, Santilli CV. Nanocrystalline anatase thin films prepared from redispersible sol–gel powders. *J Eur Ceram Soc.* 2005;25(12):2175–2180.
42. Bahadur NM, Furusawa T, Sato M, Kurayama F, Suzuki N. Rapid synthesis, characterization and optical properties of TiO_2 coated ZnO nanocomposite particles by a novel microwave irradiation method. *Mater Res Bull.* 2010;45(10):1383–1388.
43. Gaisin NK, Gnezdilov OI, Pashirova TN, et al. Micellar and liquid-crystalline properties of bicyclic fragment-containing cationic surfactant. *Colloid J.* 2010;72(6):764–770.
44. Carvalho FC, Sarmento VH, Chiavacci LA, Barbi MS, Gremião MP. Development and in vitro evaluation of surfactant systems for controlled release of zidovudine. *J Pharm Sci*. 2010;99(5):2367–2374.
45. Dong YD, Boyd BJ. Applications of X-ray scattering in pharmaceutical science. *Int J Pharm*. 2011;417(1–2):101–111.
46. Wang Z, Zhou W. Lamellar liquid crystals of Brij 97 aqueous solutions containing different additives. *J Solution Chem.* 2009;38(6):659–668.
47. Negrini R, Mezzenga R. pH-responsive lyotropic liquid crystals for controlled drug delivery. *Langmuir*. 2011;27(9):5296–5303.
48. Nguyen TH, Hanley T, Porter CJ, Boyd BJ. Nanostructured liquid crystalline particles provide long duration sustained-release effect for a poorly water soluble drug after oral administration. *J Control Release*. 2011;153(2):180–186.
49. Rossano M, Hucher N, Picard C, Colletta D, Le Foll F, Grisel M. Effects of aging on structure and stability of TiO_2 nanoparticle-containing oil-in-water emulsions. *Int J Pharm*. 2014;461(1–2):89–96.
50. Scalia S, Mezzena M, Bianchi A. Comparative evaluation of different substrates for the in vitro determination of sunscreen photostability: spectrophotometric and HPLC analyses. *Int J Cosmet Sci*. 2010;32(1):55–64.
51. Garoli D, Pelizzo MG, Nicolosi P, Peserico A, Tonin E, Alaibac M. Effectiveness of different substrate materials for in vitro sunscreen tests. *J Dermatol Sci*. 2009;56(2):89–98.
52. Diffey BL, Tanner PR, Matts PJ, Nash JF. In vitro assessment of the broad-spectrum ultraviolet protection of sunscreen products. *J Am Acad Dermatol*. 2000;43(6):1024–1035.
53. Diffey BL. A method for broad spectrum classification of sunscreens. *Int J Cosmet Sci*. 1994;16(2):47–52.
54. Nesseem D. Formulation of sunscreens with enhancement sun protection factor response based on solid lipid nanoparticles. *Int J Cosmet Sci*. 2011;33(1):70–79.
55. Manaia EB, Kaminski RCK, Soares CP, et al. Liquid crystalline formulations containing modified surface TiO_2 nanoparticles obtained by sol–gel process. *J Sol-Gel Sci Technol.* 2012;63(2):251–257.
56. Costa P, Sousa Lobo JM. Modeling and comparison of dissolution profiles. *Eur J Pharm Sci*. 2001;13(2):123–133.
57. Farkas E, Zelkó R, Németh Z, Pálinkás J, Marton S, Rácz I. The effect of liquid crystalline structure on chlorhexidine diacetate release. *Int J Pharm*. 2000;193(2):239–245.